Table 3. Changes in the mRNA profiles of the liver after CBDL+CDL in TIMP-1$^{-/-}$ mice TIMP-1$^{+/+}$ and TIMP-1$^{-/-}$ mice received CBDL+CDL.

	sham		CBDL+CDL	
	TIMP-1$^{+/+}$	TIMP-1$^{-/-}$	TIMP-1$^{+/+}$	TIMP-1$^{-/-}$
αSMA	1.00±0.64	1.04±0.30	5.43±0.98*	4.01±1.72
desmin	1.00±0.36	1.39±0.18	1.73±0.28*	1.59±0.34
vimentin	1.00±0.18	1.19±0.29	2.77±0.82*	2.05±0.86

The animals were sacrificed 7 days after the surgery. mRNA levels of αSMA, desmin, and vimentin in the livers were determined by quantitative real time RT-PCR. Results are presented as means ± SD of data collected from at least 5 independent experiments.

*P<0.05 versus sham-operated TIMP-1$^{+/+}$ mice using a 2-tailed Student's t-test.

doi:10.1371/journal.pone.0065251.t003

TIMP-1 is Induced in BDL Livers in a TNF-α-dependent Manner

After finding that collagen mRNA was not decreased in TNF-α$^{-/-}$ mice, we hypothesized that the reduced fibrosis in the mice was due to post-transcriptional effects. To elucidate the mechanisms by which TNF-α contributes to BDL-mediated liver fibrosis, we focused on TIMP-1, which is an endogenous inhibitor of MMPs. Consistent with a report indicating that a TNF-α inhibitor can prevent the increase in rat hepatic TIMP-1 by CCl_4 treatment [34], we found that CBDL+CDL increased mRNA (Figure 6A) and protein (Figure 6B) expression of TIMP-1 in the liver, and the induction was lower in TNF-α$^{-/-}$ mice than in TNF-α$^{+/+}$ mice. In contrast, gelatin zymography showed that MMP-9 (Figure 6C) and MMP-2 (data not shown) were equally activated by CBDL+CDL in both TNF-α$^{+/+}$ and TNF-α$^{-/-}$ mice. TIMP-1 positive cells were induced in the increased interstitial space around the dilated bile ducts (Figure 6D) and most of the desmin^{+} cells (a marker of HSCs) showed double staining for TIMP-1 (Figure 6E), suggesting that TIMP-1 is expressed by HSCs. In addition, TIMP-1 mRNA expression in primary cultured rat HSCs was increased by TNF-α administration (Table 2), indicating that TNF-α stimulates TIMP-1 production, as previously reported [9,19,20]. These results suggest that the TNF-α produced by BDL induces TIMP-1 in HSCs.

Fibrosis is Reduced in TIMP-1$^{-/-}$ Mice

Induction of TIMP-1, but not MMPs, was reduced in TNF-α$^{-/-}$ mice. This led to the hypothesis that insufficient TIMP-1 expression leads to increased collagen removal by MMPs in TNF-α$^{-/-}$ mice. To investigate the roles of TIMP-1 on fibrosis, we performed BDL on TIMP-1$^{-/-}$ mice. TIMP-1$^{-/-}$ mice showed a similar degree of increased liver injury and serum ALT (Figure 7A) as TIMP-1$^{+/+}$ mice at 1 day after CBDL+CDL. In addition, the increased expression levels of αSMA, desmin, and vimentin mRNA in the livers of TIMP-1$^{-/-}$ mice at 7 days after CBDL+CDL were comparable to those in TIMP-1$^{+/+}$ mice (Table 3). These results suggest that TIMP-1 does not play a role in hepatocyte cell death induced by bile acid or in activation of HSCs in CBDL+CDL mice. Surprisingly, the mortality rate of TIMP-1$^{-/-}$ mice that received CBDL+CDL was extremely high; 0% of mice remained by 21 days after the surgery (Figure 7B). Mice treated with our established model, PBDL, only showed liver injury and fibrosis in the bile duct ligated left lobe of the liver, which improved the survival rate to 100% in both the TIMP-1$^{+/+}$ and TIMP-1$^{-/-}$ mice. Therefore, we used PBDL for the TIMP-1$^{-/-}$ mice. Sirius red staining showed a smaller positive area in the ligated left lobe of the TIMP-1$^{-/-}$ mice (Figure 7C), suggesting that fibrosis is reduced by a TIMP-1 deficiency. Thus, TIMP-1 may have fibrogenic effects due to inhibition of collagen removal by MMPs.

Discussion

The present study investigated the contribution of TNF-α to the progression of fibrosis after cholestatic liver injury. The results, which indicate that TNF-α increases liver fibrosis through TIMP-1 production from HSCs, suggest novel therapeutic possibilities for treating liver fibrosis.

TNF-α has been thought to be crucial for liver injury and fibrosis by BDL because those are reduced in TNF-α$^{-/-}$ mice [8] and TNFR1$^{-/-}$ mice [9]. Gabele et al. reported that TNF-α$^{-/-}$ mice display reduced levels of serum ALT, Sirius red positive area, collagen-I protein expression, αSMA positive cells, and TGF-β mRNA in the liver after BDL [8]. After BDL, hepatocytes are exposed to elevated concentrations of bile acid, and hydrophobic bile acids lead to hepatocyte cell death [3,4] through various factors, such as reactive oxygen species (ROS) generation from mitochondria [35]. The initial hepatocyte cell death stimulates subsequent inflammatory responses, leading to further liver injury and fibrosis [36,37]. TNF-α is induced by BDL after the initial hepatocellular damage caused by bile acids, and both of bile acids and the induced TNF-α are reported to induce hepatocellular damage. Among them, the TNF-α-induced liver injury is canceled in TNF-α$^{-/-}$ mice after BDL. Because liver injury stimulates HSC activation, reduced liver injury may decrease fibrosis. However, it is still unclear whether the reduced liver fibrosis is due to a lack of fibrogenic effects of TNF-α or due to the reduced liver injury because previous reports indicate that both liver injury and fibrosis after CBDL are reduced in TNF-α$^{-/-}$ mice [8] and TNFR1$^{-/-}$ mice [9]. In contrast to those reports, our study found a reduction of liver fibrosis after CBDL+CDL in TNF-α$^{-/-}$ mice without a reduction in liver injury. This can be attributed to this study's use of CBDL+CDL, which is composed of CBDL and CDL, in contrast to the usual CBDL procedure, in which only the common bile duct is ligated, used in the previous studies. In CBDL+CDL mice, congested bile did not remain in the gall bladder, leading to the post-surgical exposure of hepatocytes to high concentrations of bile acid, which induced severe hepatocyte cell death. CBDL+CDL induced same degree of liver damage in TNF-α$^{-/-}$ compared with TNF-α$^{+/+}$ suggesting that the liver injury induced by bile acid may be severe enough to conceal TNF-α-mediated liver injury. In actuality, pretreatment with GalN exacerbated the CBDL+CDL-induced liver injury that was blunted in TNF-α$^{-/-}$ mice, indicating that TNF-α has a minor role in liver injury in CBDL+CDL mice. TNF-α$^{-/-}$ mice showed reduced fibrosis after CBDL+CDL, without reduction of liver injury and inflammatory cell infiltration or enhancement of liver regeneration, indicating a direct contribution by TNF-α to liver fibrosis in CBDL+CDL mice.

The profibrogenic effects of TNF-α in another fibrosis model, which uses CCl_4, have been reported previously, indicating that TNFR1 deficiency inhibits liver fibrosis after CCl_4 treatment, without any effects on liver injury [10,38]. TGF-β, one of the main fibrogenic factors, stimulates HSCs to induce collagen I α1 transcription [39]. However, the induction of TGF-β and collagen mRNAs after CBDL+CDL was similar in TNF-α$^{-/-}$ and TNF-α$^{+/+}$ mice. Moreover, exogenous administration of TNF-α decreased the induction of collagen α1(I) mRNA in primary cultured rat HSCs. These results suggest that TNF-α induces liver fibrosis post-transcriptionally. MMPs and their inhibitor, TIMP,

post-translationally modulate ECM remodeling, and the balance of their expression plays an important role in liver fibrosis [18]. Indeed, CBDL+CDL increased TIMP-1 expression, which can inhibit a broad range of MMPs and was attenuated by TNF-α deficiency. In addition, fibrosis in the ligated lobes of PBDL livers was reduced in TIMP-$1^{-/-}$ mice compared to that in TIMP-$1^{+/+}$ mice. Thus, insufficient TIMP-1 production is a possible explanation for the reduced fibrosis in TNF-$\alpha^{-/-}$ mice after CBDL+CDL. In contrast to our results, it has been reported that CCl_4-induced liver fibrosis and liver injury are increased in TIMP-$1^{-/-}$ mice [25]. In addition to its profibrogenic effects, TIMP-1 has a protective effect on hepatocytes [25]. Inhibition of MMPs blocks apoptosis of hepatocytes [40]. TIMP-$1^{-/-}$ mice demonstrate impaired liver injury and hepatocyte proliferation after hepatic ischemia and reperfusion [24]. Thus, deletion of TIMP-1 could accelerate liver fibrosis by increasing liver injury. Indeed, TIMP-$1^{-/-}$ mice that received CBDL+CDL showed an extremely high mortality rate, with an initial liver injury rate that was comparable to TIMP-$1^{+/+}$ mice, suggesting that TIMP-1 has roles in the BDL liver, in addition to MMP inhibition. However, our results using PBDL suggest that TIMP-1 has a profibrogenic role in cholestatic liver injury. TIMP-1 can act directly through cell surface receptors, in addition to indirectly directing cell fate through modulation of protease activity [41]. Both stimulatory [24] and inhibitory [42] effects of TIMP-1 on liver regeneration have been reported. Thus, further studies are required to investigate the multifunctional effects of TIMP-1 on liver injury and fibrosis. In addition, the mechanism of TIMP-1 up-regulation induced by TNF-α in the BDL liver is still unclear. It has been reported that activation of HSCs is accompanied by induction of TIMP-1 promoter activity and mRNA expression, and that AP-1, Pea3, and TIMP-1 element 1 are reported to be involved in transcriptional activity of the TIMP-1 promoter [43,44,45]. Moreover, TIMP-1 expression is also regulated by changes in mRNA stability [46]. Further studies are also needed to resolve this uncertainty.

In conclusion, we observed that TNF-α produced by cholestasis promoted liver fibrosis via TIMP-1 production from HSCs. Thus, targeting TNF-α and TIMP-1 may become a new therapeutic strategy for treating liver fibrosis and cholestatic liver injury.

Author Contributions

Conceived and designed the experiments: YO. Performed the experiments: YO MH. Analyzed the data: YO MH IY TS HM OK. Contributed reagents/materials/analysis tools: YO MH. Wrote the paper: YO.

References

1. Bataller R, Brenner DA (2001) Hepatic stellate cells as a target for the treatment of liver fibrosis. Semin Liver Dis 21: 437–451.
2. Park YJ, Qatanani M, Chua SS, LaRey JL, Johnson SA, et al. (2008) Loss of orphan receptor small heterodimer partner sensitizes mice to liver injury from obstructive cholestasis. Hepatology 47: 1578–1586.
3. Jang JH, Rickenbacher A, Humar B, Weber A, Raptis DA, et al. (2012) Serotonin protects mouse liver from cholestatic injury by decreasing bile salt pool after bile duct ligation. Hepatology 56: 209–218.
4. Sokol RJ, Devereaux M, Dahl R, Gumpricht E (2006) "Let there be bile"–understanding hepatic injury in cholestasis. J Pediatr Gastroenterol Nutr 43 Suppl 1: S4–9.
5. Higuchi H, Gores GJ (2003) Bile acid regulation of hepatic physiology: IV. Bile acids and death receptors. Am J Physiol Gastrointest Liver Physiol 284: G734–738.
6. Schwabe RF, Brenner DA (2006) Mechanisms of Liver Injury. I. TNF-alpha-induced liver injury: role of IKK, JNK, and ROS pathways. Am J Physiol Gastrointest Liver Physiol 290: G583–589.
7. Bemelmans MH, Gouma DJ, Greve JW, Buurman WA (1992) Cytokines tumor necrosis factor and interleukin-6 in experimental biliary obstruction in mice. Hepatology 15: 1132–1136.
8. Gabele E, Froh M, Arteel GE, Uesugi T, Hellerbrand C, et al. (2009) TNFalpha is required for cholestasis-induced liver fibrosis in the mouse. Biochem Biophys Res Commun 378: 348–353.
9. Tarrats N, Moles A, Morales A, Garcia-Ruiz C, Fernandez-Checa JC, et al. (2011) Critical role of tumor necrosis factor receptor 1, but not 2, in hepatic stellate cell proliferation, extracellular matrix remodeling, and liver fibrogenesis. Hepatology 54: 319–327.
10. Sudo K, Yamada Y, Moriwaki H, Saito K, Seishima M (2005) Lack of tumor necrosis factor receptor type 1 inhibits liver fibrosis induced by carbon tetrachloride in mice. Cytokine 29: 236–244.
11. Nagaki M, Sugiyama A, Osawa Y, Naiki T, Nakashima S, et al. (1999) Lethal hepatic apoptosis mediated by tumor necrosis factor receptor, unlike Fas-mediated apoptosis, requires hepatocyte sensitization in mice. J Hepatol 31: 997–1005.
12. Osawa Y, Nagaki M, Banno Y, Yamada Y, Imose M, et al. (2001) Possible involvement of reactive oxygen species in D-galactosamine-induced sensitization against tumor necrosis factor-alpha-induced hepatocyte apoptosis. J Cell Physiol 187: 374–385.
13. Nagaki M, Naiki T, Brenner DA, Osawa Y, Imose M, et al. (2000) Tumor necrosis factor alpha prevents tumor necrosis factor receptor-mediated mouse hepatocyte apoptosis, but not fas-mediated apoptosis: role of nuclear factor-kappaB. Hepatology 32: 1272–1279.
14. Yamada Y, Kirillova I, Peschon JJ, Fausto N (1997) Initiation of liver growth by tumor necrosis factor: deficient liver regeneration in mice lacking type I tumor necrosis factor receptor. Proc Natl Acad Sci U S A 94: 1441–1446.
15. Varela-Rey M, Fontan-Gabas L, Blanco P, Lopez-Zabalza MJ, Iraburu MJ (2007) Glutathione depletion is involved in the inhibition of procollagen alpha1(I) mRNA levels caused by TNF-alpha on hepatic stellate cells. Cytokine 37: 212–217.
16. Hernandez-Munoz I, de la Torre P, Sanchez-Alcazar JA, Garcia I, Santiago E, et al. (1997) Tumor necrosis factor alpha inhibits collagen alpha 1(I) gene expression in rat hepatic stellate cells through a G protein. Gastroenterology 113: 625–640.
17. Houglum K, Buck M, Kim DJ, Chojkier M (1998) TNF-alpha inhibits liver collagen-alpha 1(I) gene expression through a tissue-specific regulatory region. Am J Physiol 274: G840–847.
18. Arthur MJ (2000) Fibrogenesis II. Metalloproteinases and their inhibitors in liver fibrosis. Am J Physiol Gastrointest Liver Physiol 279: G245–249.
19. Tomita K, Tamiya G, Ando S, Ohsumi K, Chiyo T, et al. (2006) Tumour necrosis factor alpha signalling through activation of Kupffer cells plays an essential role in liver fibrosis of non-alcoholic steatohepatitis in mice. Gut 55: 415–424.
20. Knittel T, Mehde M, Kobold D, Saile B, Dinter C, et al. (1999) Expression patterns of matrix metalloproteinases and their inhibitors in parenchymal and non-parenchymal cells of rat liver: regulation by TNF-alpha and TGF-beta1. J Hepatol 30: 48–60.
21. Roderfeld M, Weiskirchen R, Wagner S, Berres ML, Henkel C, et al. (2006) Inhibition of hepatic fibrogenesis by matrix metalloproteinase-9 mutants in mice. Faseb J 20: 444–454.
22. Parsons CJ, Bradford BU, Pan CQ, Cheung E, Schauer M, et al. (2004) Antifibrotic effects of a tissue inhibitor of metalloproteinase-1 antibody on established liver fibrosis in rats. Hepatology 40: 1106–1115.
23. Yoshiji H, Kuriyama S, Miyamoto Y, Thorgeirsson UP, Gomez DE, et al. (2000) Tissue inhibitor of metalloproteinases-1 promotes liver fibrosis development in a transgenic mouse model. Hepatology 32: 1248–1254.
24. Duarte S, Hamada T, Kuriyama N, Busuttil RW, Coito AJ (2012) TIMP-1 deficiency leads to lethal partial hepatic ischemia and reperfusion injury. Hepatology 56: 1074–1085.
25. Wang H, Lafdil F, Wang L, Yin S, Feng D, et al. (2011) Tissue inhibitor of metalloproteinase 1 (TIMP-1) deficiency exacerbates carbon tetrachloride-induced liver injury and fibrosis in mice: involvement of hepatocyte STAT3 in TIMP-1 production. Cell Biosci 1: 14.
26. Osawa Y, Seki E, Adachi M, Taura K, Kodama Y, et al. (2006) Systemic mediators induce fibrogenic effects in normal liver after partial bile duct ligation. Liver Int 26: 1138–1147.
27. Osawa Y, Seki E, Adachi M, Suetsugu A, Ito H, et al. (2010) Role of acid sphingomyelinase of Kupffer cells in cholestatic liver injury in mice. Hepatology 51: 237–245.
28. Osawa Y, Suetsugu A, Matsushima-Nishiwaki R, Yasuda I, Saibara T, et al. (2013) Liver acid sphingomyelinase inhibits growth of metastatic colon cancer. J Clin Invest.
29. Osawa Y, Uchinami H, Bielawski J, Schwabe RF, Hannun YA, et al. (2005) Roles for C16-ceramide and sphingosine 1-phosphate in regulating hepatocyte apoptosis in response to tumor necrosis factor-alpha. J Biol Chem 280: 27879–27887.
30. Osawa Y, Hannun YA, Proia RL, Brenner DA (2005) Roles of AKT and sphingosine kinase in the antiapoptotic effects of bile duct ligation in mouse liver. Hepatology 42: 1320–1328.

31. Osawa Y, Banno Y, Nagaki M, Nozawa Y, Moriwaki H, et al. (2001) Caspase activation during hepatocyte apoptosis induced by tumor necrosis factor-alpha in galactosamine-sensitized mice. Liver 21: 309–319.
32. Reeves HL, Dack CL, Peak M, Burt AD, Day CP (2000) Stress-activated protein kinases in the activation of rat hepatic stellate cells in culture. J Hepatol 32: 465–472.
33. Schwabe RF, Bataller R, Brenner DA (2003) Human hepatic stellate cells express CCR5 and RANTES to induce proliferation and migration. Am J Physiol Gastrointest Liver Physiol 285: G949–958.
34. Roderfeld M, Geier A, Dietrich CG, Siewert E, Jansen B, et al. (2006) Cytokine blockade inhibits hepatic tissue inhibitor of metalloproteinase-1 expression and up-regulates matrix metalloproteinase-9 in toxic liver injury. Liver Int 26: 579–586.
35. Yerushalmi B, Dahl R, Devereaux MW, Gumpricht E, Sokol RJ (2001) Bile acid-induced rat hepatocyte apoptosis is inhibited by antioxidants and blockers of the mitochondrial permeability transition. Hepatology 33: 616–626.
36. Jaeschke H (2002) Inflammation in response to hepatocellular apoptosis. Hepatology 35: 964–966.
37. Canbay A, Higuchi H, Bronk SF, Taniai M, Sebo TJ, et al. (2002) Fas enhances fibrogenesis in the bile duct ligated mouse: a link between apoptosis and fibrosis. Gastroenterology 123: 1323–1330.
38. Simeonova PP, Gallucci RM, Hulderman T, Wilson R, Kommineni C, et al. (2001) The role of tumor necrosis factor-alpha in liver toxicity, inflammation, and fibrosis induced by carbon tetrachloride. Toxicol Appl Pharmacol 177: 112–120.
39. Bataller R, Brenner DA (2005) Liver fibrosis. J Clin Invest 115: 209–218.
40. Wielockx B, Lannoy K, Shapiro SD, Itoh T, Itohara S, et al. (2001) Inhibition of matrix metalloproteinases blocks lethal hepatitis and apoptosis induced by tumor necrosis factor and allows safe antitumor therapy. Nat Med 7: 1202–1208.
41. Stetler-Stevenson WG (2008) Tissue inhibitors of metalloproteinases in cell signaling: metalloproteinase-independent biological activities. Sci Signal 1: re6.
42. Mohammed FF, Pennington CJ, Kassiri Z, Rubin JS, Soloway PD, et al. (2005) Metalloproteinase inhibitor TIMP-1 affects hepatocyte cell cycle via HGF activation in murine liver regeneration. Hepatology 41: 857–867.
43. Iredale JP, Benyon RC, Arthur MJ, Ferris WF, Alcolado R, et al. (1996) Tissue inhibitor of metalloproteinase-1 messenger RNA expression is enhanced relative to interstitial collagenase messenger RNA in experimental liver injury and fibrosis. Hepatology 24: 176–184.
44. Bahr MJ, Vincent KJ, Arthur MJ, Fowler AV, Smart DE, et al. (1999) Control of the tissue inhibitor of metalloproteinases-1 promoter in culture-activated rat hepatic stellate cells: regulation by activator protein-1 DNA binding proteins. Hepatology 29: 839–848.
45. Trim JE, Samra SK, Arthur MJ, Wright MC, McAulay M, et al. (2000) Upstream tissue inhibitor of metalloproteinases-1 (TIMP-1) element-1, a novel and essential regulatory DNA motif in the human TIMP-1 gene promoter, directly interacts with a 30-kDa nuclear protein. J Biol Chem 275: 6657–6663.
46. Doyle GA, Saarialho-Kere UK, Parks WC (1997) Distinct mechanisms regulate TIMP-1 expression at different stages of phorbol ester-mediated differentiation of U937 cells. Biochemistry 36: 2492–2500.

Research article

Liver acid sphingomyelinase inhibits growth of metastatic colon cancer

Yosuke Osawa,[1,2,3] Atsushi Suetsugu,[2] Rie Matsushima-Nishiwaki,[1] Ichiro Yasuda,[2] Toshiji Saibara,[4] Hisataka Moriwaki,[2] Mitsuru Seishima,[3] and Osamu Kozawa[1]

[1]Department of Pharmacology, [2]Department of Gastroenterology, and [3]Department of Informative Clinical Medicine, Gifu University Graduate School of Medicine, Gifu, Japan. [4]Department of Gastroenterology and Hepatology, Kochi University School of Medicine, Kochi, Japan.

Acid sphingomyelinase (ASM) regulates the homeostasis of sphingolipids, including ceramides and sphingosine-1-phosphate (S1P). These sphingolipids regulate carcinogenesis and proliferation, survival, and apoptosis of cancer cells. However, the role of ASM in host defense against liver metastasis remains unclear. In this study, the involvement of ASM in liver metastasis of colon cancer was examined using *Asm*$^{-/-}$ and *Asm*$^{+/+}$ mice that were inoculated with SL4 colon cancer cells to produce metastatic liver tumors. *Asm*$^{-/-}$ mice demonstrated enhanced tumor growth and reduced macrophage accumulation in the tumor, accompanied by decreased numbers of hepatic myofibroblasts (hMFs), which express tissue inhibitor of metalloproteinase 1 (TIMP1), around the tumor margin. Tumor growth was increased by macrophage depletion or by *Timp1* deficiency, but was decreased by hepatocyte-specific ASM overexpression, which was associated with increased S1P production. S1P stimulated macrophage migration and TIMP1 expression in hMFs in vitro. These findings indicate that ASM in the liver inhibits tumor growth through cytotoxic macrophage accumulation and TIMP1 production by hMFs in response to S1P. Targeting ASM may represent a new therapeutic strategy for treating liver metastasis of colon cancer.

Introduction

Colon cancer, one of the most common malignancies, frequently metastasizes to the liver. Acid sphingomyelinase (ASM) is involved in various physiological cellular functions and diseases, including cancer (1), and hydrolyzes sphingomyelin into ceramide and phosphorylcholine. Ceramide, a bioactive mediator of numerous cellular functions, such as apoptosis and cell cycle regulation (2, 3), is in turn hydrolyzed by ceramidase into sphingosine, which is subsequently phosphorylated into sphingosine-1-phosphate (S1P) by sphingosine kinase (SphK). Although these sphingolipids are involved in colon carcinogenesis and colon cancer cell survival (4, 5), the roles of ASM and S1P in host antitumor defenses (i.e., inhibiting the progression of colon cancer metastasis to the liver) remain unclear.

Tumors contain stromal cells, such as immune cells and fibroblasts (6). Infiltrated tumor-associated macrophages (TAMs) have recently been reported to function as promoters of tumor progression (7–9), with several clinical studies demonstrating an association between the presence of TAMs and poor prognosis in various cancers (10). In contrast, opposing data have shown that the presence of TAMs is correlated with improved survival and that these cells have protective potential in colon cancer (11, 12). Although tumor growth–promoting TAMs have been observed to resemble regulatory M2 macrophages (13, 14), the density of classically activated M1 macrophages is positively correlated with the survival time of patients with non–small-cell lung cancer (15). These findings indicate that macrophages have contrasting roles in cancer, depending on their phenotype (13).

S1P is a ceramide-derived metabolite that is involved in various cellular functions and increases migration of macrophages (16, 17), resulting in macrophage recruitment. S1P released from apoptotic tumor cells induces a switch from the M1 to the M2 macrophage subtype (18). In contrast, the S1P analog FTY720 does not alter the ratio of M1 and M2 subtypes in mouse peritoneal macrophages (19). Because of these contrasting findings, the effect of S1P on macrophages remains controversial and poorly understood. Whereas MMP cleavage of the ECM, a primary barrier against tumor invasion produced by hepatic myofibroblasts (hMFs) in the liver, promotes cancer cell migration, invasion, and metastasis, MMP inhibitors reduce colon cancer metastasis to the liver (20). Specifically, overexpression of tissue inhibitors of metalloproteinases (TIMPs), endogenous inhibitors of MMPs, inhibits liver metastasis of colon cancer in animal models (21), whereas decreased TIMP1 expression in the liver results in progression of SV40T antigen–induced hepatocellular carcinoma (22) and increased metastatic colonization of T cell lymphoma (23). However, it has been reported that elevated TIMP levels are associated with cancer progression (24). Thus, although S1P stimulates hMF accumulation and TIMP1 induction in the liver (25, 26), the precise roles of S1P in tumor growth remain unclear. To attempt to clarify these precise roles, we here investigated the involvement of ASM in the progression of liver metastasis of colon cancer.

Results

Role of ASM deficiency and overexpression in the progression of metastatic liver tumors of colon cancer. To determine the role of host ASM on metastatic liver tumor growth caused by colon cancer, we created metastatic liver tumors by intrasplenic injection with SL4 cells, a mouse colon cancer cell line, and examined expression of ASM and ceramide by immunostaining. ASM and ceramide expression increased in the liver cells around the tumors (Supplemental Figure 1A; supplemental material available online with this article; doi:10.1172/JCI65188DS1), which suggests that tumor cells stimulate ASM expression and promote its activity in liver cells. To examine the effect of ASM deficiency on metastatic liver tumors, the extent of tumor growth in *Asm*$^{+/+}$ and *Asm*$^{-/-}$ mice

Conflict of interest: The authors have declared that no conflict of interest exists.
Citation for this article: *J Clin Invest.* 2013;123(2):834–843. doi:10.1172/JCI65188.

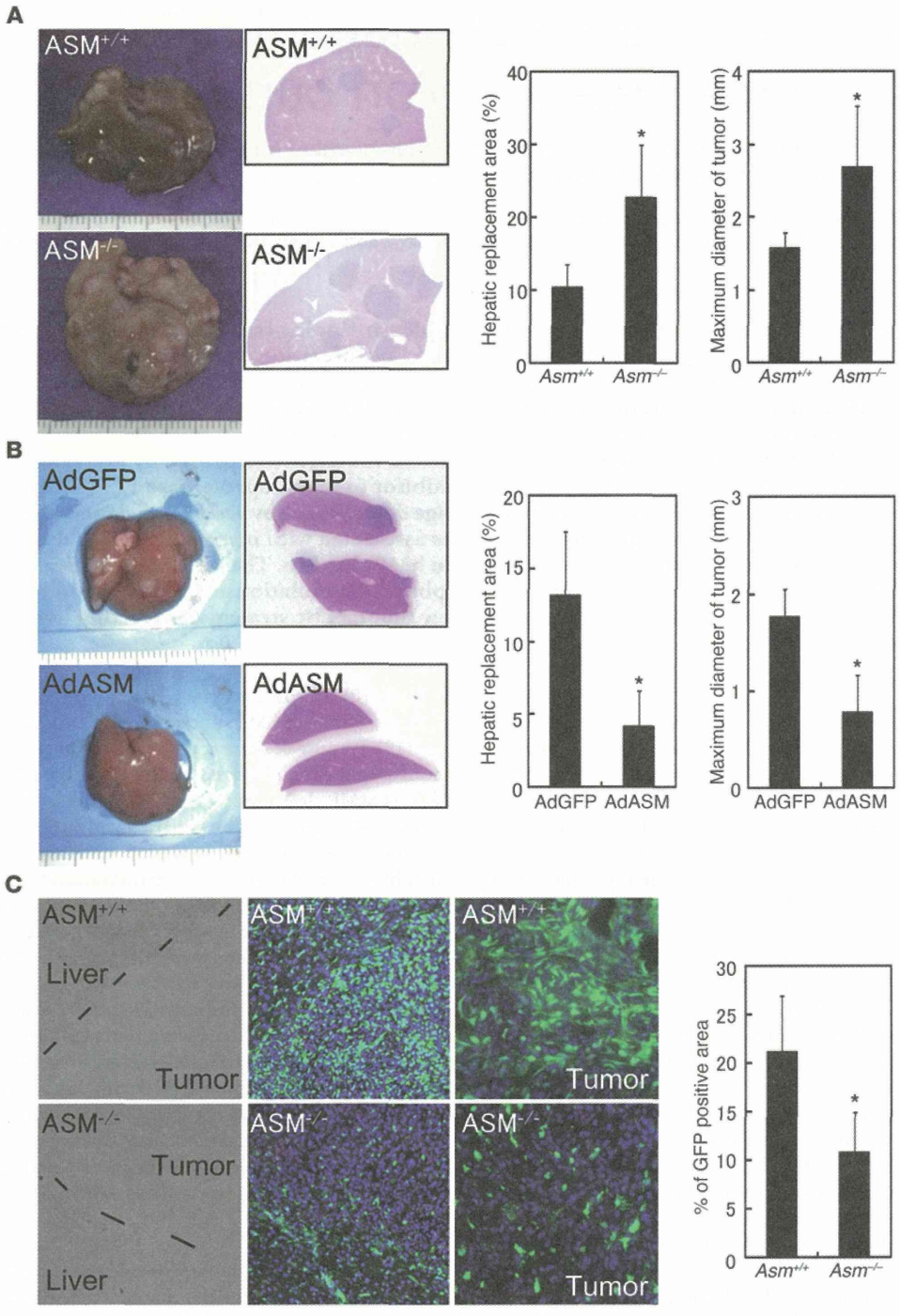

Figure 1
ASM deficiency increased, and ASM overexpression decreased, metastatic tumor growth in the liver. (**A** and **B**) $Asm^{+/+}$ and $Asm^{-/-}$ mice were intrasplenically injected with 2×10^4 SL4 cells (**A**). Wild-type mice were infected with AdGFP or AdASM 24 hours before inoculation (**B**). Mice were sacrificed 14 days after inoculation, and livers were excised and photographed. Liver sections were stained with H&E (loupe magnification), and intrahepatic tumor load was presented as hepatic replacement area and maximum diameter, based on measurement of 3 nonsequential sections. (**C**) $GFP^+Asm^{+/+}$ and $GFP^+Asm^{-/-}$ mice were intrasplenically injected with SL4 cells. At 14 days after inoculation, GFP expression in the liver was assessed by fluorescent microscopy, measurement of the GFP^+ area was performed, and nuclei were stained with DAPI. Shown are bright field images at the border of the metastatic tumor and liver (left), GFP/DAPI merge in the same bright field images (middle), and higher-magnification views of GFP/DAPI merge in the tumor area (right). Original magnification, ×200 (left and middle); ×400 (right). Results are mean ± SD of data obtained from at least 5 independent experiments. $^*P < 0.05$, 2-tailed Student's *t* test.

was compared. No tumors were evident in livers without SL4 cell inoculation (Supplemental Figure 1B). After inoculation with SL4 cells, the hepatic replacement area, maximum tumor diameter, and liver weight were increased in $Asm^{-/-}$ compared with $Asm^{+/+}$ mice (Figure 1A and Supplemental Figure 1C). In contrast, a similar number of the initially transplanted cells was observed in the livers of $Asm^{+/+}$ and $Asm^{-/-}$ mice 6 hours after inoculation (Supplemental Figure 2A). These results indicate that colon cancer cells grow more rapidly in the $Asm^{-/-}$ liver. Conversely, administration of adenovirus-expressing ASM (AdASM) to the mice prior to cancer cell inoculation inhibited tumor growth compared with adenovirus-expressing GFP (AdGFP) administration (Figure 1B). AdASM-derived GFP was expressed in the hepatocytes, but not in the tumor cells (Supplemental Figure 2B). In support of the results of our previous study (27), AdASM increased ASM activity in the liver (Supplemental Figure 2C). In addition, ASM-chimeric mice,

in which ASM was deficient only in bone marrow–derived cells, demonstrated tumor growth that was comparable to mice containing $Asm^{+/+}$ bone marrow cells (Supplemental Figure 3A). These results indicate that ASM in hepatocytes, but not in bone marrow–derived cells, is involved in the inhibition of tumor growth.

To explore the mechanisms of enhanced tumor growth in $Asm^{-/-}$ mice, we generated $GFP^{+}Asm^{-/-}$ mice and examined the host-tumor interaction by inoculating $GFP^{+}Asm^{+/+}$ and $GFP^{+}Asm^{-/-}$ mice with SL4 cells. After inoculation, spindle-shaped host-derived GFP^{+} cells, most of which expressed F4/80 (Figure 2A), were observed in the metastatic liver tumors, while fewer host-derived cell infiltrates were observed in the $Asm^{-/-}$ livers (Figure 1C). Spindle-shaped bone marrow–derived cells were also observed in the tumors of GFP-chimeric mice (expressing GFP only in bone marrow–derived cells; Supplemental Figure 3B), which suggests that these cells were $F4/80^{+}$ macrophages originating from the bone marrow. $F4/80^{+}$ cells were observed in the tumors; compared with the control livers, a smaller number of $F4/80^{+}$ cells was observed in the $Asm^{-/-}$ livers, while a greater number of these cells was present in AdASM-infected livers (Figure 2, B and C). The induction of classically activated M1 macrophage markers (*Cd11c*, *Il12p40*, and *Ifng*) by SL4 cell inoculation was more remarkable than that of *Cd163*, mannose receptor, and *Il10*, markers for regulatory M2 macrophages (Supplemental Table 1). Thus, these findings suggested that the accumulated macrophages were M1 dominant. In $Asm^{+/+}$ mice transplanted with $GFP^{+}Asm^{-/-}$ bone marrow, the number of bone marrow–derived $GFP^{+}Asm^{-/-}$ cells in the tumor was comparable to that of $GFP^{+}Asm^{+/+}$ cells in the control $Asm^{+/+}$ mice transplanted with $GFP^{+}Asm^{+/+}$ bone marrow (Supplemental Figure 3C). Therefore, it is likely that ASM in hepatocytes, but not in bone marrow–derived cells, contributes to the accumulation of macrophages in tumors.

To examine whether macrophage accumulation in tumors is involved in the inhibition of tumor growth, liposome-encapsulated alendronate was administered to the SL4 cell–inoculated mice to decrease the number of $F4/80^{+}$ cells in the tumors (Supplemental Figure 3D). Alendronate administration increased the severity of tumor growth by inducing macrophage depletion (Figure 2D), which is suggestive of macrophage involvement in tumor growth suppression. These data indicate that hepatocytic ASM leads to accumulation of antitumor macrophages in the metastatic liver tumors of colon cancer, thereby suppressing tumor growth.

Macrophage-induced hMFs accumulate around invasive margins of metastatic liver tumors. Macrophages have been shown to exhibit antitumor potential as tumoricidal cells and major antigen-presenting cells (28–31). Liver macrophages also modulate the host immune response to cancer cells by releasing cytotoxic products and immune-stimulating factors, including IFN-γ. In accordance with these findings, $CD3^{+}$ lymphocytes infiltrated into the tumors, and fewer $CD3^{+}$ cells were observed in $Asm^{-/-}$ and alendronate-treated mice (Supplemental Figure 4, A and B). Moreover, a NKT cell activator, α-galactosylceramide, suppressed tumor growth, even in $Asm^{-/-}$ mice (Supplemental Figure 4C), which suggests that the antitumor immunity of NKT cells was not impaired in $Asm^{-/-}$ mice. Thus, NKT cells contributed to the antitumor defense mechanism.

Activated macrophages release various types of inflammatory cytokines and growth factors. Among these, TNF-α is thought to induce tumor necrosis. However, in the model used in this study, mRNA expression of *Tnfa* was comparable in SL4 cell–inoculated $Asm^{-/-}$ and $Asm^{+/+}$ livers (Supplemental Table 2), and tumor growth was not increased in $Tnfa^{-/-}$ mice (Supplemental Figure 4D), which suggests that TNF-α is not involved in tumor development in $Asm^{-/-}$ mice. The reduced induction of *Il1b*, *Cxcl1*, and *Tgfb* mRNA expression by SL4 cell inoculation in $Asm^{-/-}$ compared with $Asm^{+/+}$ livers (Supplemental Table 2) can be explained by the reduction in the number of macrophages in the $Asm^{-/-}$ liver, as these factors are released from liver macrophages. The mRNA expression levels of *Des* (encoding desmin, a marker of hMFs), *Acta2* (encoding α-SMA, a marker of activated hMFs), and *Col1a1* (encoding collagen α1[I], a product of activated hMFs) were also increased after SL4 cell inoculation in $Asm^{+/+}$ livers (Supplemental Table 2), which suggests that the metastatic tumors stimulated hMF proliferation and activation. In the SL4 cell–inoculated mice, the number of $desmin^{+}$ and $\alpha\text{-SMA}^{+}$ cells were increased around the invasive margins of the tumors in the liver (Figure 3). $Desmin^{+}$ cells were observed to express GFP in the GFP^{+} mice, but not in the GFP-chimeric mice (data not shown), which suggests that the hMFs were derived from host, not from bone marrow. The increase of *Des*, *Acta2*, and *Col1a1* mRNA after SL4 cell inoculation was lower in $Asm^{-/-}$ than in $Asm^{+/+}$ livers (Supplemental Table 2). Moreover, whereas the number of $desmin^{+}$ and $\alpha\text{-SMA}^{+}$ cells was decreased by *Asm* deficiency (Figure 3A) and by macrophage depletion (Figure 3C), it was increased by ASM overexpression (Figure 3B). These findings suggest that increased macrophage accumulation in the metastatic liver tumor by ASM stimulates hMF accumulation and activation. Because the number of $desmin^{+}$ and $\alpha\text{-SMA}^{+}$ cells was inversely correlated with tumor growth, we concluded that hMFs may contribute to tumor suppression.

Role of TIMP1 produced by hMFs in growth suppression of metastatic liver tumors. Although it has been reported that hMFs contribute to cancer progression, the model used in this study indicated that increased hMF accumulation is negatively correlated with tumor growth. This finding led us to hypothesize that hMFs contain antitumor factors that are increased in number and magnitude by ASM overexpression and decreased by ASM deficiency. To test this hypothesis, we focused on examining TIMP1, which exhibits antitumor potential (21) and is expressed by hMFs (32). In the metastatic tumors, most of the $desmin^{+}$ cells showed double staining for TIMP1 (Figure 4A), which suggests that hMFs are $TIMP1^{+}$. *Timp1* mRNA expression increased in $Asm^{+/+}$ livers by SL4 cell inoculation, an increase that was attenuated in $Asm^{-/-}$ livers (Figure 4B). Nevertheless, the expression levels of *Mmp2*, *Mmp9*, and *Mmp13* were comparable in $Asm^{+/+}$ and $Asm^{-/-}$ livers (Supplemental Table 2). The increased number of $TIMP1^{+}$ cells observed around the invasive margin of the tumors was attenuated by *Asm* deficiency as well as by macrophage depletion (Figure 4, C and E), whereas ASM overexpression further increased $TIMP1^{+}$ cell number (Figure 4D), similar to our findings with respect to hMF induction. These results, in addition to the increased tumor growth observed in $Timp1^{-/-}$ mice (Figure 4F), suggest that the increased expression of TIMP1 in hMFs by metastatic tumors is involved in the suppression of tumor growth.

ASM suppression of tumor growth via S1P production. In accordance with previous reports that ASM hydrolyzes sphingomyelin into ceramide, which is then hydrolyzed by ceramidase and phosphorylated by SphK to form S1P, we observed the level of S1P to increase in AdASM-infected livers (Figure 5A). Although exogenous administration of S1P did not affect *Tnfa*, *Il1b*, *Cxcl1*, *Tgfb*, *Il12p40*, or *Il10* mRNA expression in isolated peritoneal $CD11b^{+}$ macrophages (Supplemental Table 3), these cells showed increased migration toward S1P (Figure 5B), as previously reported regarding RAW 264.7 macrophages (33). These findings suggest that macrophage accumulation in tumors might be caused by S1P-induced macrophage recruitment. Although it

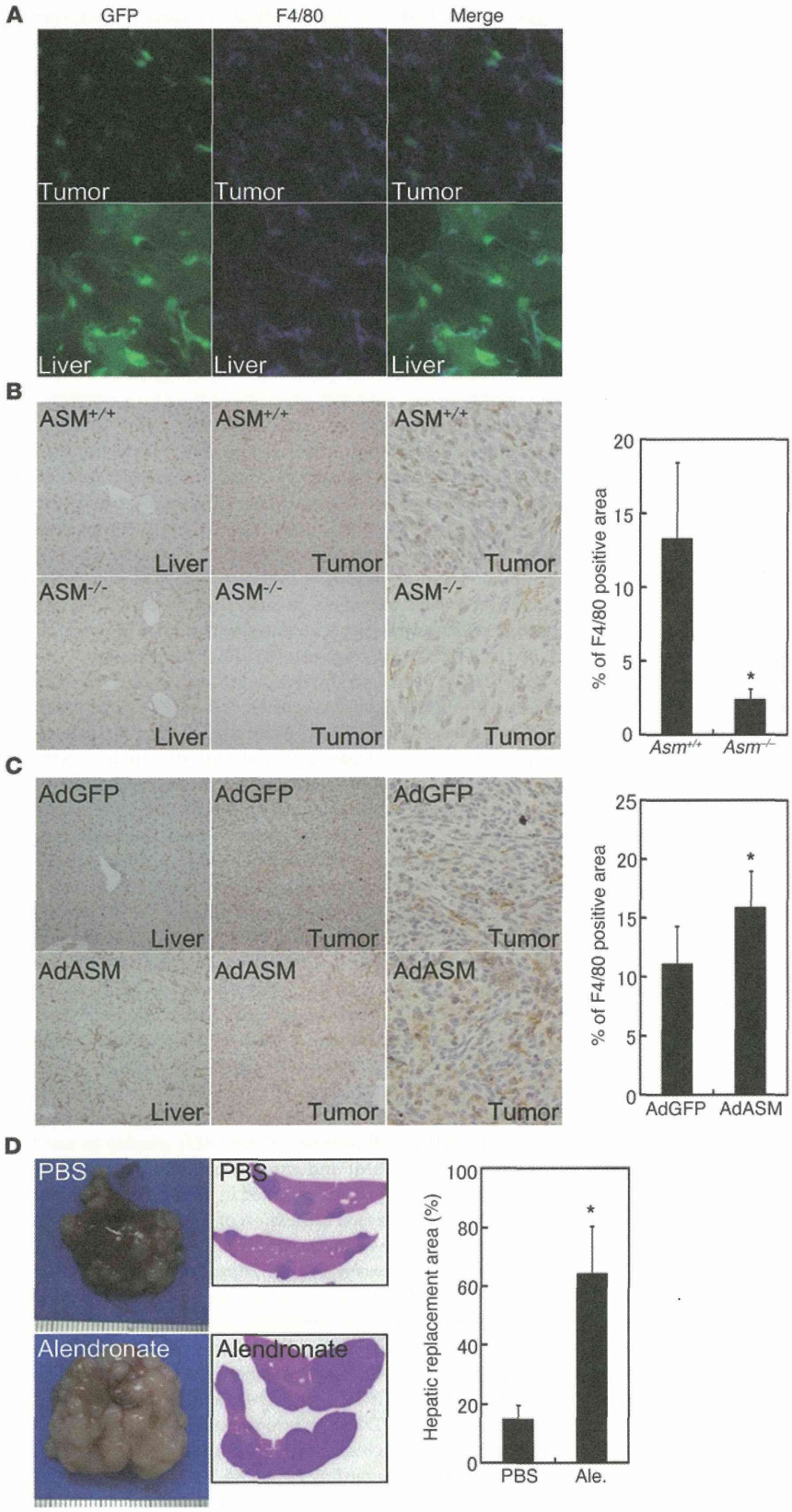

Figure 2

Macrophage depletion increased metastatic tumor growth in the liver. (**A**) *GFP*+ mice were intrasplenically injected with 2 × 10^4 SL4 cells. GFP fluorescence was visualized with fluorescent microscopy, and macrophages were detected in metastatic tumor and liver by immunofluorescent staining for F4/80 (blue). Original magnification, ×400. (**B** and **C**) *Asm*$^{+/+}$ and *Asm*$^{-/-}$ mice (**B**) and AdGFP- and AdASM-infected wild-type mice (**C**) were intrasplenically injected with 2 × 10^4 SL4 cells. Expression of F4/80 in the liver and metastatic tumor was examined by immunohistochemistry with an anti-F4/80 antibody to assess the number of macrophages. Original magnification, ×100 (left and middle); ×400 (right). (**D**) Wild-type mice were injected with SL4 cells and treated with PBS or alendronate before sacrifice 14 days after inoculation. Images of livers after excision and liver sections stained with H&E (loupe magnification) are shown. Intrahepatic tumor load is presented as hepatic replacement area, based on measurement of 3 nonsequential sections. Results are mean ± SD of data collected from at least 5 independent experiments. *$P < 0.05$, 2-tailed Student's *t* test.

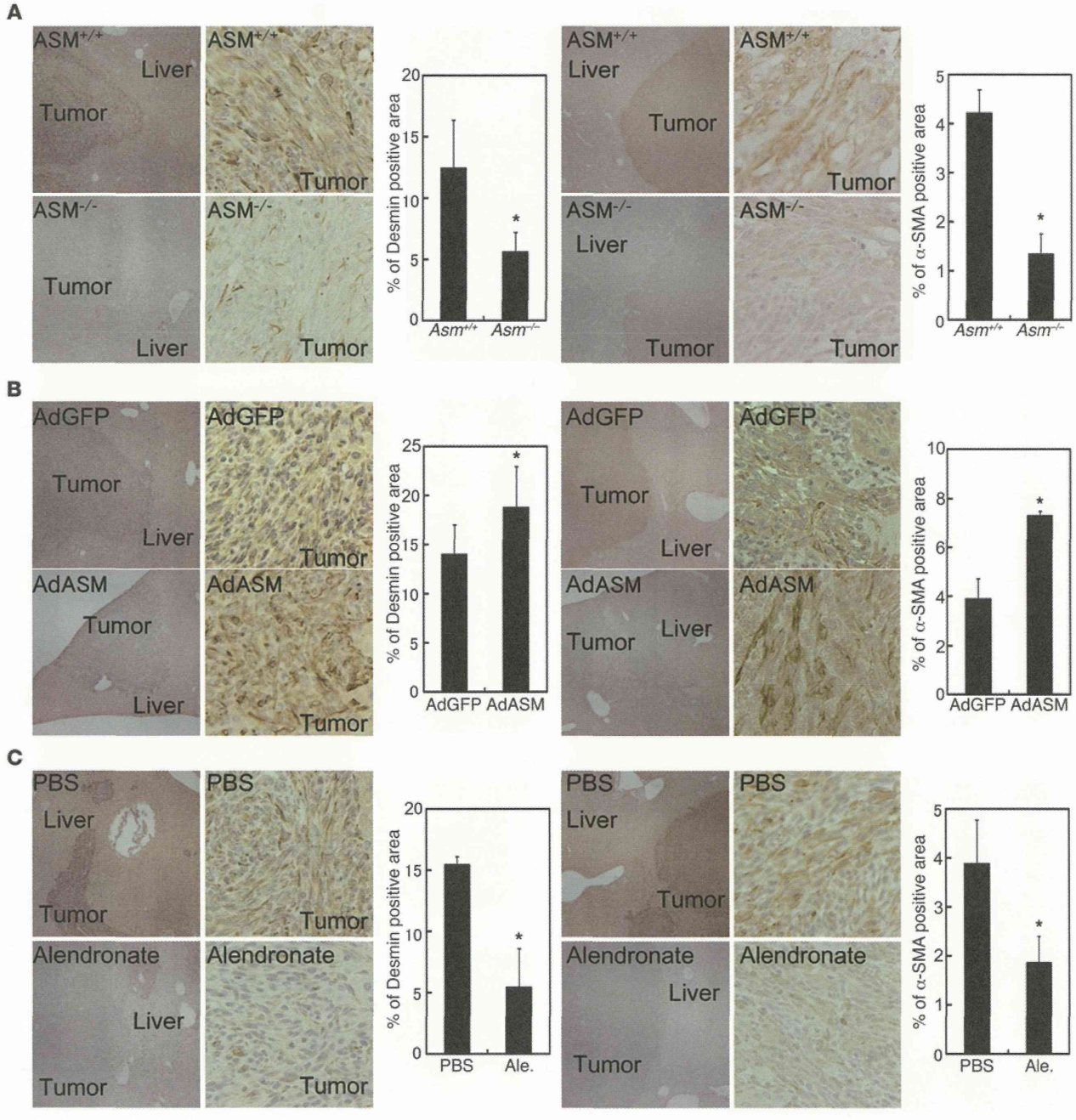

Figure 3

ASM deficiency or macrophage depletion decreased hMFs, and ASM overexpression increased hMFs, around the tumor invasive margin. *Asm*$^{+/+}$ and *Asm*$^{-/-}$ mice (**A**), AdGFP- or AdASM-infected wild-type mice (**B**), and wild-type mice treated with PBS or alendronate (**C**) were intrasplenically injected with 2×10^4 SL4 cells and sacrificed 14 days after inoculation. Expression of desmin (left) and α-SMA (right) around the tumor invasive margin was examined by immunohistochemistry, and measurement of immunostain-positive area was performed. Original magnification, ×40 (left); ×400 (right). Results are mean ± SD of data collected from at least 5 independent experiments. *$P < 0.05$, 2-tailed Student's *t* test.

has been reported that S1P induces a switch from the M1 to the M2 macrophage subtype (18), in the present study, S1P did not alter the mRNA expression levels of M1 and M2 markers, which suggests that S1P does not affect the macrophage phenotype. Instead, our observations that 1 μM S1P treatment for 72 hours increased *Timp1* mRNA expression in isolated hMFs (Figure 5C) and that adenoviral overexpression of SphK1 (AdSphK) in hepatocytes prior to cancer cell inoculation inhibited tumor growth (Supplemental Figure 5A) suggest that ASM suppresses tumor growth via S1P production. The fold increase of *Timp1* mRNA induced by S1P did not seem to

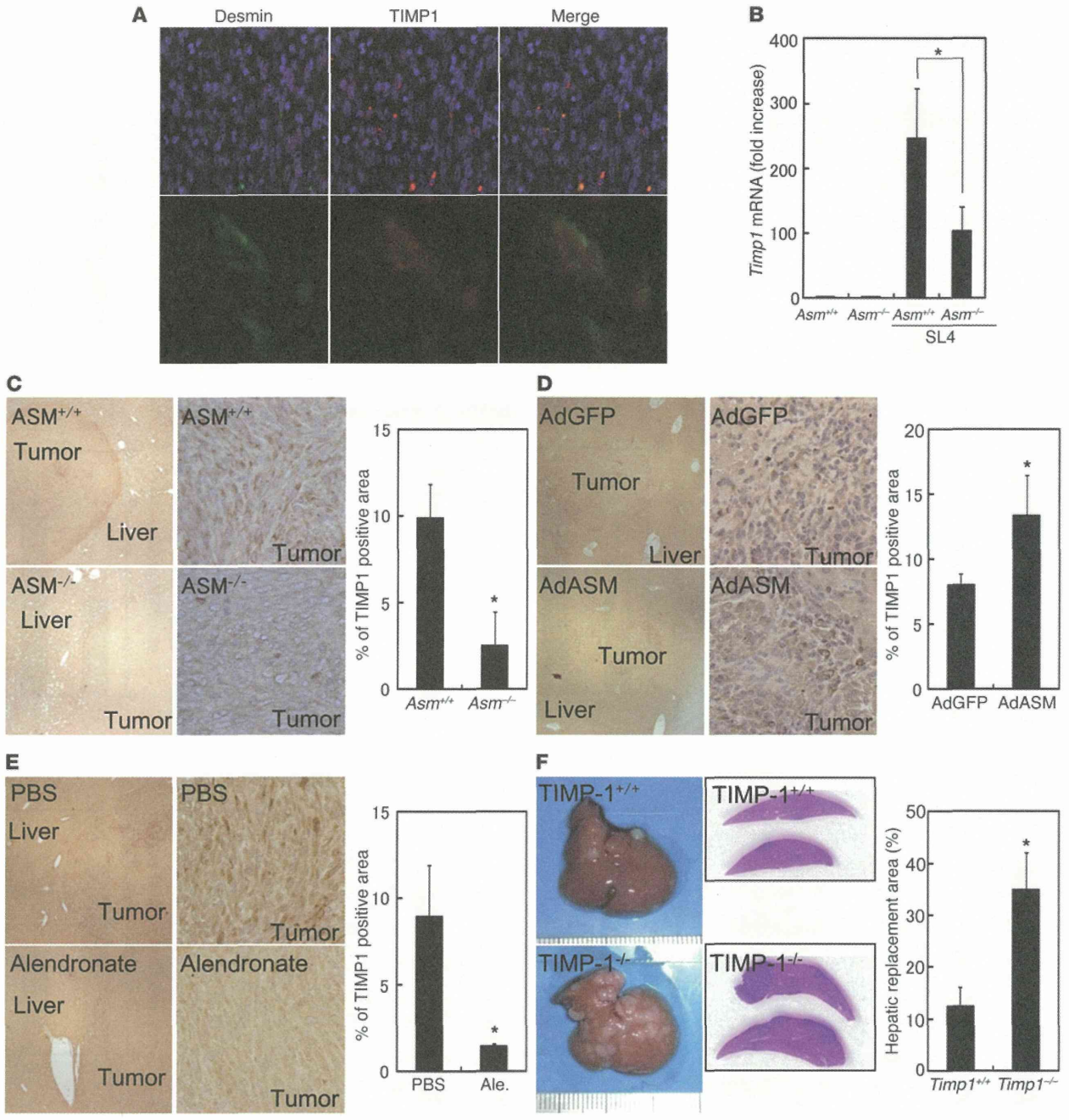

Figure 4

TIMP1 deficiency increased metastatic tumor growth in the liver. (**A**) Wild-type mice were intrasplenically injected with 2×10^4 SL4 cells and sacrificed 14 days after inoculation. Expression of desmin (green) and TIMP1 (red) around the invasive margin of the tumors was examined by immunofluorescent staining. Nuclei were stained with DAPI (blue, top). Original magnification, ×400 (top); ×1,600 (bottom). (**B**) *Asm*$^{+/+}$ and *Asm*$^{-/-}$ mice were intrasplenically injected with 5×10^5 SL4 cells and sacrificed 7 days after inoculation. *Timp1* mRNA expression in the liver was determined by quantitative real-time RT-PCR. (**C**–**E**) *Asm*$^{+/+}$ and *Asm*$^{-/-}$ mice (**C**), AdGFP- or AdASM-infected wild-type mice (**D**), and wild-type mice treated with PBS or alendronate (**E**) were intrasplenically injected with 2×10^4 SL4 cells and sacrificed 14 days after inoculation. TIMP1 expression around the tumor invasive margin was examined by immunohistochemistry, and measurement of TIMP1$^+$ area was performed. Original magnification, ×40 (left); ×400 (right). (**F**) *Timp1*$^{+/+}$ and *Timp1*$^{-/-}$ mice were intrasplenically injected with 2×10^4 SL4 cells and sacrificed 14 days after inoculation. Images of livers after excision and liver sections stained with H&E (loupe magnification) are shown. Intrahepatic tumor load is presented as hepatic replacement area, based on measurement of 3 nonsequential sections. Results are mean ± SD of data collected from at least 5 independent experiments. *$P < 0.05$, 2-tailed Student's *t* test.

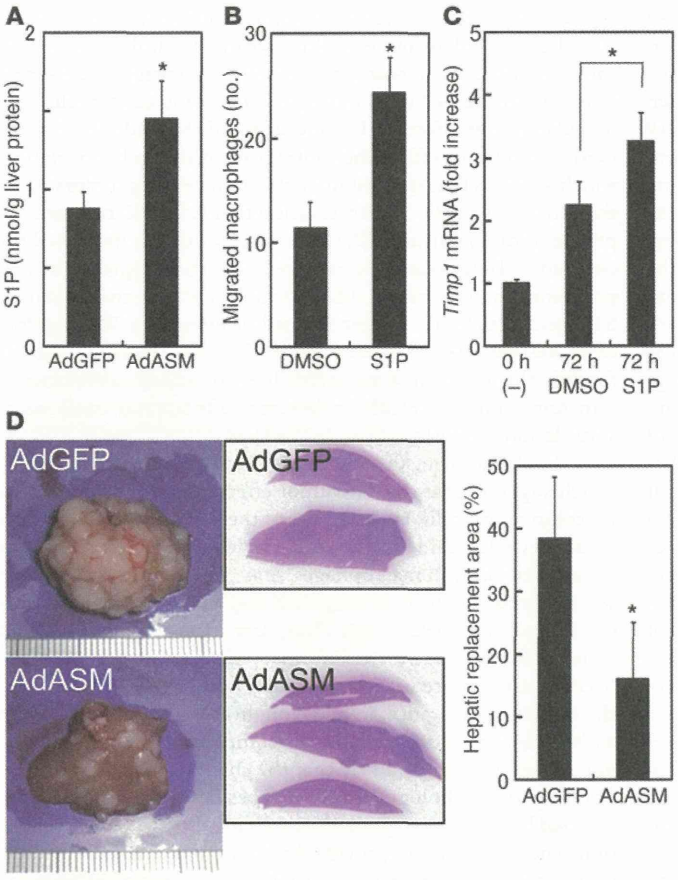

Figure 5

S1P promoted macrophage migration and *Timp1* mRNA expression in hMFs. (**A**) Wild-type mice were infected with AdGFP or AdASM, and S1P was examined by MS analysis 3 days after infection. (**B**) After addition of CD11b$^+$ peritoneal macrophages and 1 μM S1P to the upper and lower chambers, respectively, of transwell plates, cells were incubated for 4 hours. The number of macrophages that migrated to the underside of the chamber was determined. (**C**) Primary rat hMFs were incubated with or without 1 μM S1P on plastic dishes for 72 hours before determination of *Timp1* mRNA levels by quantitative real-time RT-PCR. (**D**) Wild-type mice were intrasplenically injected with 2×10^4 SL4 cells, infected with AdGFP or AdASM 5 days after inoculation, and sacrificed 14 days after infection (i.e., 19 days after inoculation). Images of livers after excision and liver sections stained with H&E (loupe magnification) are shown. Intrahepatic tumor load is presented as hepatic replacement area, based on measurement of 3 nonsequential sections. Results are mean ± SD of data collected from 4 (**A**) or at least 5 (**B**–**D**) independent experiments. *$P < 0.05$, 2-tailed Student's *t* test.

be large (Figure 5C). However, a 48-hour treatment with TGF-β has previously been reported to induce an approximately 2-fold increase of *TIMP1* mRNA in cultured human hMFs (34). This suggests that the induction of *Timp1* mRNA by S1P was not a small change, and it is possible that the induction might be sufficient. 5 μM S1P induced TIMP1 expression to a similar degree as that observed using 1 μM S1P (data not shown), which suggests that 1 μM S1P fully induces activation of S1P receptors.

As described above, ASM exerted an antitumor effect through macrophage accumulation and TIMP1 production from hMFs via S1P. To evaluate AdASM administration as a form of treatment against metastatic liver tumors of colon cancer, AdASM was administered to mice 5 days after SL4 cell inoculation. AdASM suppressed tumor growth, even when it was administered after cell inoculation (Figure 5D). However, AdSphK administration did not suppress tumor growth (Supplemental Figure 5B), although the accumulation of F4/80$^+$ and desmin$^+$ cells was similar to that in AdASM-treated mice (Supplemental Figure 6A). In addition, accumulation of F4/80$^+$ and desmin$^+$ cells was observed to be equal, regardless of whether mice were infected with AdSphK before or after SL4 cell inoculation (data not shown). Adenovirus-mediated GFP expression was observed in the tumors when the virus was administered after cell inoculation (Supplemental Figure 6B), which suggests that the adenovirus infects not only hepatocytes, but also inoculated SL4 cells. The observation that AdSphK increased proliferation of cultured SL4 cells (Supplemental Figure 6C) indicated that the antitumor effects of overexpressed SphK1 in the liver may be counteracted by the tumor-promoting effects of SphK1 on SL4 cell proliferation.

Discussion

In the present study, we investigated the contribution of ASM to the suppression of tumor growth in liver metastasis of colon cancer cells. Our results indicated that liver ASM inhibits tumor growth through S1P formation and subsequent macrophage accumulation and TIMP1 production from hMFs. These results suggest novel therapeutic possibilities for treating metastatic liver tumors of colon cancer.

ASM in cancer cells is involved in cell death and plays an important role in the host response to a variety of anticancer treatments, including those for colon cancer (1). In the present study, metastatic tumors of colon cancer cells stimulated ASM expression and ceramide in liver cells. Moreover, host ASM deficiency increased, while overexpression of ASM in the liver decreased, the growth of liver tumors after inoculation with colon cancer cells, which suggests that ASM in host cells contributes to antitumor defense. Among the roles that ASM plays in liver cells, ASM in hepatocytes stimulates glucose uptake, resulting in improvement of glucose tolerance in mice through S1P production (27). ASM has pleiotropic signaling functions related to posttranslational processing of ASM, and secretory and lysosomal ASM (35) may have distinct functions. Although it is unclear which type of ASM was